











ORIGINAL ARTICLE

Inhibition of acid ceramidase elicits mitochondrial dysfunction and oxidative stress in pancreatic cancer cells

Tomohiko Tanai^{1,2}  | Yoshihiro Shirai^{1,2}  | Yohta Shimada² | Ryoga Hamura^{1,2}  | Mitsuru Yanagaki^{1,2}  | Naoki Takada^{1,2}  | Takashi Horiuchi^{1,2} | Koichiro Haruki^{1,2}  | Kenei Furukawa^{1,2}  | Tadashi Uwagawa¹ | Kazuhito Tsuboi³ | Yasuo Okamoto³ | Shu Shimada⁴  | Shinji Tanaka⁴  | Toya Ohashi² | Toru Ikegami¹ 

¹Department of Surgery, The Jikei University School of Medicine, Tokyo, Japan

²Division of Gene Therapy, Research Center for Medical Science, The Jikei University School of Medicine, Tokyo, Japan

³Department of Pharmacology, Kawasaki Medical School, Kurashiki, Japan

⁴Department of Molecular Oncology Graduate School of Medicine, Tokyo Medical and Dental University, Tokyo, Japan

Correspondence

Yoshihiro Shirai, The Jikei University School of Medicine, 3-25-8 Nishi-Shinbashi, Minato-ku, Tokyo 105-8461, Japan.
Email: shirai@jikei.ac.jp

Funding information

Japan Society for the Promotion of Science KAKENHI, Grant/Award Number: 17K16584, 20K17665; Uehara Memorial Foundation; Jikei University.

Abstract

Although the inhibition of acid ceramidase (AC) is known to induce antitumor effects in various cancers, there are few reports in pancreatic cancer, and the underlying mechanisms remain unclear. Moreover, there is currently no safe administration method of AC inhibitor. Here the effects of gene therapy using siRNA and shRNA for AC inhibition with its mechanisms for pancreatic cancer were investigated. The inhibition of AC by siRNA and shRNA using an adeno-associated virus 8 (AAV8) vector had antiproliferative effects by inducing apoptosis in pancreatic cancer cells and xenograft mouse model. Acid ceramidase inhibition elicits mitochondrial dysfunction, reactive oxygen species accumulation, and manganese superoxide dismutase suppression, resulting in apoptosis of pancreatic cancer cells accompanied by ceramide accumulation. These results elucidated the mechanisms underlying the antitumor effect of AC inhibition in pancreatic cancer cells and suggest the potential of the AAV8 vector to inhibit AC as a therapeutic strategy.

KEYWORDS

acid ceramidase, adeno-associated virus, mitochondrial dysfunction, oxidative stress, pancreatic ductal adenocarcinoma

1 | INTRODUCTION

Impaired metabolism of various sphingolipids, such as sphingomyelin, ceramide, and sphingosine-1-phosphate, has been associated with several human diseases, including type 2 diabetes mellitus, Alzheimer's disease, and numerous cancers.¹ Sphingolipids, which are cell membrane

components, play important roles in the growth and proliferation of cancer cells.² The sphingolipid ceramide is known to induce cell apoptosis³ and improve sensitivity to chemotherapy.⁴ Therefore, targeting of ceramides has been used in several cancer treatment strategies.

The ceramide metabolic pathway includes various enzymes, such as sphingomyelinase⁵ and neutral ceramidase,⁶ which have been identified

Abbreviations: AAV8, adeno-associated virus serotype 8; AC, acid ceramidase; ALT, alanine aminotransferase; AST, aspartate aminotransferase; DW, distilled water; EGFP, enhanced green fluorescent protein; GAPDH, glyceraldehyde 3-phosphate dehydrogenase; GEM, gemcitabine; LC-MS/MS, liquid chromatography-tandem mass spectrometry; MIF, mean intensity of fluorescence; MMP, mitochondrial membrane potential; MnSOD, manganese superoxide dismutase; NAC, N-acetylcysteine; NT, non-treatment; PARP, cleaved poly(adenosine diphosphate-ribose) polymerase; PBS, phosphate-buffered saline; ROS, reactive oxygen species; SDS, sodium dodecyl sulfate; shRNA, short hairpin RNA; siRNA, small interfering RNA.

This is an open access article under the terms of the Creative Commons Attribution-NonCommercial-NoDerivs License, which permits use and distribution in any medium, provided the original work is properly cited, the use is non-commercial and no modifications or adaptations are made.

© 2021 The Authors. *Cancer Science* published by John Wiley & Sons Australia, Ltd on behalf of Japanese Cancer Association.

as therapeutic targets for ceramide accumulation in cancers. Acid ceramidase, a lysosomal enzyme that hydrolyzes ceramide into sphingosine and fatty acids,⁷ has recently attracted increasing attention for the treatment of various cancers.^{8,9} Acid ceramidase is the causative enzyme of Farber disease,¹⁰ a lysosome storage disorder associated with a poor prognosis, and the inhibition of this enzyme is reported to induce apoptosis of various cancer cells.⁸ Furthermore, AC inhibition was reported to increase radiosensitivity in prostate cancer,¹¹ improve chemosensitivity in the head and neck cancers,¹² and induce antitumor effects in glioblastoma.¹³ However, the effect of AC inhibition against pancreatic cancer remains unclear. A previous study¹⁴ using a cell culture system and ceramide analogs on pancreatic cancer was reported, but the detailed molecular biochemical mechanism underlying ceramide-induced cell apoptosis was not elucidated. Therefore, further clarification of the effect of AC inhibition and the underlying mechanism in pancreatic cancer is expected to contribute to the development of new therapeutic methods.

Novel AC inhibitors are required for the development of therapeutic strategies against pancreatic cancer. Some AC inhibitors, such as N-oleoylethanolamine,¹⁵ LCL521,¹⁶ and ARN14899,¹⁷ have been evaluated in preclinical trials but have not yet been applied clinically. Carmofur, an oral drug reported to improve the prognosis of patients with colon cancer,¹⁸ was approved for the treatment of colon and breast cancers in Japan in 1981,⁸ and is the only AC inhibitor clinically available.¹⁹ However, its application is limited due to risk of leukoencephalopathy,²⁰ which has prevented the approval of this drug by the US FDA.⁸ In addition, the insolubility of carmofur prevents intravenous administration.¹⁹ Thus, there is currently no safe administration method. For these reasons, it is important to develop a novel therapeutic technique for AC inhibition.

Therefore, the present study aimed to investigate the efficacy of gene therapy using siRNA and shRNA to block AC in pancreatic cancer. Moreover, the antitumor mechanisms underlying AC inhibition are partially elucidated.

2 | MATERIALS AND METHODS

2.1 | Cell lines

The human pancreatic cancer cell lines PANC-1 (cell number I-4446) and MIA PaCa-2 (cell number I-4311) were purchased from the Cell Resource Center for Biomedical Research, Institute of Development, Aging and Cancer, Tohoku University. PATC66 were a kind gift from Dr Paul J. Chiao, The University of Texas, MD Anderson Cancer Center. PANC-1 and MIA PaCa-2 were maintained in DMEM containing 10% FBS and 1% penicillin/streptomycin. RPMI-1640 medium was used for PATC66. All cells were incubated under a humidified atmosphere of 5% CO₂/95% air at 37°C.

2.2 | Reagents

Gemcitabine (Eli Lilly Japan) was dissolved in DW and stored at -20°C until use. N-acetylcysteine (FUJIFILM Wako Pure Chemical

Corporation) was dissolved in DMSO and stored at -20°C until use. ¹⁴C-labeled C12 ceramide was chemically prepared from sphingosine (Enzo Life Sciences) and [1-¹⁴C]lauric acid (Moravek Biochemicals) as previously described for N-[¹⁴C]oleoylsphingosine.²¹

2.3 | Antibodies

Monoclonal antibodies specific to cleaved caspase-3 (#9664), cleaved caspase-8 (#9496), cleaved PARP (#9546), GAPDH (#2118), and phospho-Akt (#4060) were obtained from Cell Signaling Technology. A mAb specific to AC (sc136275) was purchased from Santa Cruz Biotechnology, and MnSOD (ab68155) was obtained from Abcam.

2.4 | Small interfering RNA transfection

Small interfering RNA against AC (siGENOME SMART pool; M-005228-01-0005), siGENOME AC-Set of four Upgrade (MU-005228-01-0002), and its nontargeting control (siScr, siGENOME nontargeting siRNA pool #1; D-001206-13-20) were purchased from Horizon Discovery. The target sequences of siAC-Set of four Upgrade were as follows: siAC I, CACCAUAAAUCUUGACUUA; siAC II, GGUCAUAACUGAGCAACUA; siAC III, UAUUAUGAACUCGAUGCUGAA; and siAC IV, GAAAUAAGCACAAGUUAUG. The cultured cells were transfected with each siRNA using Lipofectamine RNAiMAX Transfection Reagent (Thermo Fisher Scientific) in accordance with the manufacturer's protocols.

2.5 | Plasmid transfection

For overexpression of AC, the cDNA encoding human AC²² was inserted into the pEF6/Myc-His mammalian expression vector at the *KpnI* and *BamHI* sites. The MIA PaCa-2 cells were then transfected with this plasmid DNA using Lipofectamine 2000 Transfection Reagent (Thermo Fisher Scientific) in accordance with the manufacturer's protocols.

2.6 | Experimental treatment groups

To evaluate the antitumor effects, the cells were divided into four treatment groups: siScr + DW, siAC + DW, siScr + GEM, and siAC + GEM. To assess the role of ROS in the antitumor effect, the cells were divided into three treatment groups: siScr, siAC, and siAC + NAC. The NAC concentration was 5 mmol/L in accordance with the protocol of the CellROX Deep Red Flow Cytometry Assay Kit (Thermo Fisher Scientific).

2.7 | Adeno-associated virus serotype 8

In a xenograft mouse model, a mammalian shRNA knock-down AAV8 vector (VectorBuilder) was used with either shAC or

scramble shRNA, together with EGFP. The target sequence of AC was GGTCATAACTGAGCAACTAACTCGAGTTTAGTTGCTCAGTTATGACC. A detailed map of the vector is presented in Figure S1. The scramble vector VB180117-102Oznr was purchased from VectorBuilder. The experiments using AAV vectors were approved by the Recombinant Gene Safety Committee of Jikei University (approval no. R1-18-2) and the Committee for Laboratory Biosafety of Jikei University (approval no. II-1-52).

2.8 | Animal experimental protocol

A pancreatic cancer xenograft mouse model was created by subcutaneous injection of 5×10^6 PANC-1 cells suspended in 100 μ L PBS in 4-week-old male mice (BALB/c nu/nu). When the average tumor major axis reached 8 mm, the mice were randomly divided into two groups, AAV8-shScr and AAV8-shAC. Vectors encoding 2×10^{11} genome copies suspended in 20 μ L PBS were directly injected into the subcutaneous tumor. The mice were killed when the tumor length reached 20 mm. Tumor volume was calculated as follows: (major axis) \times (minor axis) \times (minor axis)/2 (mm^3). The protocol for this animal experiment was approved by the Institutional Animal Care and Use Committee of Jikei University (approval no. 2019-015). The study was carried out in accordance with the Guidelines for the Proper Conduct of Animal Experiments of the Science Council of Japan based on the Declaration of Helsinki.

2.9 | Western blot analysis

Protein extraction and western blot analysis were undertaken as described in a previous study.²³ After incubating the blots with each primary Ab (1:200 dilution for AC and 1:1000 dilution for others) for 24 hours (48 hours for AC), the membranes were incubated with secondary Abs (1:10 000 dilution; Histofine; Nichirei Bioscience). The protein bands were enhanced with Clarity Max (Bio-Rad Laboratories).

2.10 | Acid ceramidase enzymatic activity assay

The premix preparation and enzymatic reaction were undertaken as previously described,²² except that the reaction time was extended from 30 minutes to 2 hours in some experiments. Thin-layer chromatography was carried out at 4°C for 20 minutes with a mixture of chloroform / methanol / acetic acid (94:1:5, by volume). To calculate the enzymatic activities, the radioactivities of the substrate and product on the plate were quantified using an image analyzer (Typhoon 9400; GE Healthcare) and a shield box made of lead to increase the sensitivity of enzyme assays.

2.11 | Apoptosis analysis via flow cytometry

The Annexin V/FITC Kit (Miltenyi Biotec) was utilized to stain cultured cells, which were analyzed using the Attune NxT Flow

Cytometer (Thermo Fisher Scientific) to evaluate the induction of apoptosis in accordance with the manufacturers' protocols.

2.12 | Cell proliferation assay

PANC-1, PATC66 (2×10^3 cells/well), and MIA PaCa-2 (1×10^3 cells/well) cells were seeded into the wells of 96-well plates and transfected with siRNA as described above. Cell proliferation was measured using the CCK-8 (Dojindo Laboratories) in accordance with the manufacturer's protocols.

2.13 | Liquid chromatography-tandem mass spectrometry analysis of intracellular ceramide

Cells were homogenized with 100 μ L distilled water. Cell lysate (50 μ L) was mixed with 45 pmol C17-ceramide (860517P; Avanti Polar Lipids) as an internal control, and 1 mL extraction buffer (chloroform : methanol = 2:1), and the mixture was shaken for 30 minutes at room temperature. After centrifugation for 10 minutes, the lower layer was collected, 10 μ L of which was analyzed by HPLC equipped with a triple quadrupole mass spectrometer (LCMS-8040; Shimadzu). A Synergi MAX-RP (150 mm \times 4.6 mm; Phenomenex) was used for separation. The flow rate was 0.4 mL/min. Mobile phase A was distilled water (Kanto Chemical) containing 2 mmol/L ammonium acetate (FUJIFILM Wako Pure Chemical Corporation) and 0.1% formic acid (Nacalai Tesque). Mobile phase B consisted of methanol (FUJIFILM Wako Pure Chemical Corporation) including 2 mmol/L ammonium acetate and 0.1% formic acid. The mobile phase gradients were as follows: 0-0.01 minute, 10% B; 0.01-1 minute, 10%-50% B; 1-1.01 minute, 100% B; 1.01-30 minutes, 100% B; and 30.01-30.5 minutes, 0% B. Ceramide isoforms were quantified by multiple reaction monitoring in positive ion mode. Transitions are listed below: C16 (d18:1/16:0); m/z 538.2 > 264.2, C18 (d18:1/18:0); m/z 566.55 > 264.2, C24 (d18:1/24:0); m/z 650.45 > 264.25, C17 (d18:1/17:0); and m/z 552.45 > 264.2. The concentrations of those isoforms were calculated by using a calibration curve of ceramide (860052P; Avanti Polar Lipids).

2.14 | Mitochondrial membrane potential analysis

The MMP was evaluated using the JC-1 MitoMP Detection Kit (Dojindo Laboratories) in accordance with the manufacturer's protocols. The stained cells were detected using a fluorescence microscope, and quantitative analyses were undertaken using an Attune NxT Flow Cytometer (Thermo Fisher Scientific).

2.15 | Quantitative analysis of intracellular ROS

The cells (1×10^5 cells) were seeded into a 100-mm dish transfected with siRNA 12 hours later. After transfection for 24 hours,

the medium was changed, and the cells were treated with or without NAC for 72 hours. Subsequently, the cells were stained using the CellROX Deep Red Flow Cytometry Assay Kit (Thermo Fisher Scientific) to assess the induction of ROS and analyzed using an Attune NxT Flow Cytometer (Thermo Fisher Scientific) in accordance with the manufacturer's protocols.

2.16 | Analysis of mitochondria-derived ROS

MitoSOX Red Mitochondrial Superoxide Indicator (Thermo Fisher Scientific) was used in accordance with the manufacturer's protocols. The cells were stained with MitoTracker and MitoSOX Red and observed under a fluorescence microscope. Quantitative analyses were carried out using an Attune NxT Flow Cytometer (Thermo Fisher Scientific).

2.17 | Statistical analysis

Data are expressed as mean \pm SD. As for tumor volume, data are expressed as mean \pm SE. Comparisons were carried out using the two-tailed nonpaired *t* test or repeated measures ANOVA as appropriate. A *P* value of less than .05 was considered statistically significant. The log-rank test was used to evaluate overall survival in xenograft mouse model.

3 | RESULTS

3.1 | Knockdown of AC induces antiproliferative effects in pancreatic cancer cells and tumors

The AC levels of PANC-1, PATC66, and MIA PaCa-2 cells were determined by western blot analysis (Figure 1A,B). The results indicated that the AC expression was high in PANC-1 cells, moderate in PATC66 cells, and low in MIA PaCa-2 cells. After western blot analysis, enzymatic activity analysis, and quantitative analysis of intracellular ceramide, LC-MS/MS was used to determine whether AC was actually knocked down by siRNA and whether AC suppression induced the accumulation of intracellular ceramide, which is known to induce cell apoptosis.²⁴ In all cell lines, siAC transfection suppressed AC expression (Figure 1C,D). The enzymatic activity of AC was significantly suppressed in all cell lines (Figure 1E). Acid ceramidase inhibition increased the intracellular levels of C16, C18, and C24 ceramides in all cell lines (Figure 1F). Following siScr transfection, the intracellular level of ceramide was lower than that of the nontreatment group. These results indicate that siAC inhibited the functional activity of AC and induced the intracellular accumulation of several ceramide species.

Next, the effect of AC knockdown on cell proliferation and apoptosis induction was evaluated. In all cell lines (PANC-1, PATC66, and MIA PaCa-2), proliferation was suppressed by AC

inhibition (Figure 2A). Western blot analysis was used to evaluate the expression levels of the apoptosis markers caspase-8, cleaved caspase-3, and cleaved PARP to investigate the effects of AC knockdown on apoptosis of pancreatic cancer cells. The results revealed that AC knockdown increased the levels of all apoptosis markers (Figure 2B,C). Moreover, the results of the annexin assay indicated an increase in the proportion of apoptotic cells in the siAC group (Figure 2D). Furthermore, an AAV8-shAC vector (Figure S1) was generated to evaluate the antitumor effect of AC knockdown in a xenograft mouse model. The target sequence of AC was determined by western blot analysis and LC-MS/MS analysis of intracellular ceramide using siGENOME AC-Set of four Upgrade (Figure S2), and the sequence with the highest efficiency for the accumulation of ceramide was selected. The function of the AAV vector was confirmed by western blot analysis, a cell proliferation assay, and fluorescence microscopy for the detection of EGFP (Figure S3). The tumor volume was significantly smaller, and overall survival was significantly longer in the AAV8-shAC group compared with those of the AAV8-shScr group (Figure 2E,F). The side-effects of AAV8 and AAV8-shAC were also evaluated, which revealed no significant difference in the body weight or blood data, such as AST and ALT, between the treatment (AAV8-shScr and AAV8-shAC) and control (nontreatment) groups (Figure 2G,H). These results indicated that AC suppression had antiproliferative effects by inducing apoptosis of pancreatic cancer cells and tumors.

3.2 | Inhibition of AC induces mitochondrial dysfunction accompanied by ROS accumulation resulting in cell apoptosis

Ceramide is involved in cell death and tumor suppression through mitochondrial dysfunction.^{25,26} Thus, the MMP following AC knockdown was analyzed using the fluorescent dye JC-1 to evaluate the effect of ceramide accumulation on mitochondrial function. JC-1 fluorescence changes from red to green upon MMP depolarization. The results revealed that AC knockdown increased the proportion of green fluorescence cells in all cell lines (Figure 3A,B). These data indicate that AC inhibition elicits mitochondrial dysfunction.

To elucidate the mechanisms underlying cell apoptosis by AC inhibition, the levels of intracellular ROS, which is mainly generated by dysfunctional mitochondria, were measured.²⁷ First, ROS was quantified by flow cytometry, which indicated that AC inhibition generated high levels of ROS in all cell lines (Figure 3C). Next, fluorescent staining showed that AC knockdown induced mitochondrial generation of ROS (Figure 3D). Contrarily, NAC reduced the generation of siAC-induced ROS (Figure 3C). Similarly, NAC canceled cell apoptosis induced by AC knockdown, indicating that the accumulation of ROS causes cell apoptosis (Figure 3E). These results suggest that the generation of ROS due to ceramide accumulation by AC knockdown was the main cause of cell apoptosis. We also used overexpression model of AC in MIA PaCa-2 cells in which AC was knocked down to validate the AC functions regarding the mitochondrial dysfunction

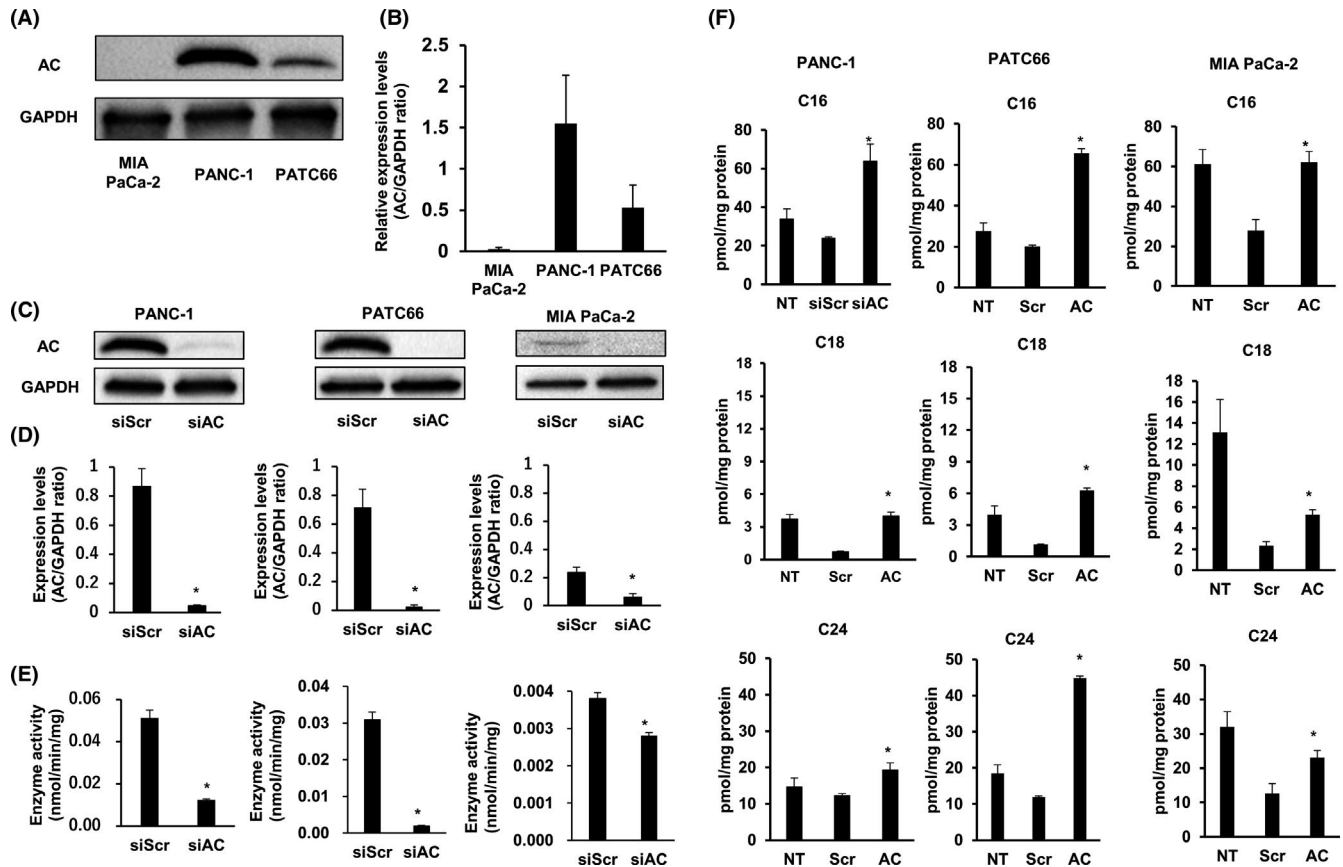


FIGURE 1 Relative expression levels of acid ceramidase (AC) in pancreatic cancer cells. A, Western blot analysis. B, Densitometry obtained from triplicate western blots. AC was certainly knocked down by siRNA. C, D, In all cell lines, siRNA against AC (siAC) transfection suppressed AC expression ($*P < .01$; $n = 3$). E, The enzymatic activity of AC was significantly suppressed in all cell lines ($*P < .01$; $n = 3$). F, Quantitative analysis of intracellular ceramide. The amount of intracellular ceramide was increased in each cell line after 72 h ($*P < .01$; $n = 3$). NT, no treatment

and oxidative stress. Acid ceramidase overexpression in these cells revealed ceramide degradation, resulting in the recovery of mitochondrial membrane potential and reduction of ROS (Figure S4). These results reinforced that AC affected mitochondrial function and oxidative stress.

Moreover, the effects of AC knockdown on the activities of the ROS scavenger MnSOD were investigated. An interesting report noted that ROS activated Akt, which resulted in the downregulation of MnSOD.²⁸ The results of the present study revealed that AC knockdown enhanced p-Akt expression while decreasing the MnSOD expression (Figure 3F), suggesting that ROS accumulation induced by mitochondrial dysfunction was further enhanced by MnSOD suppression.

3.3 | Acid ceramidase suppression and GEM have additive effects on apoptosis

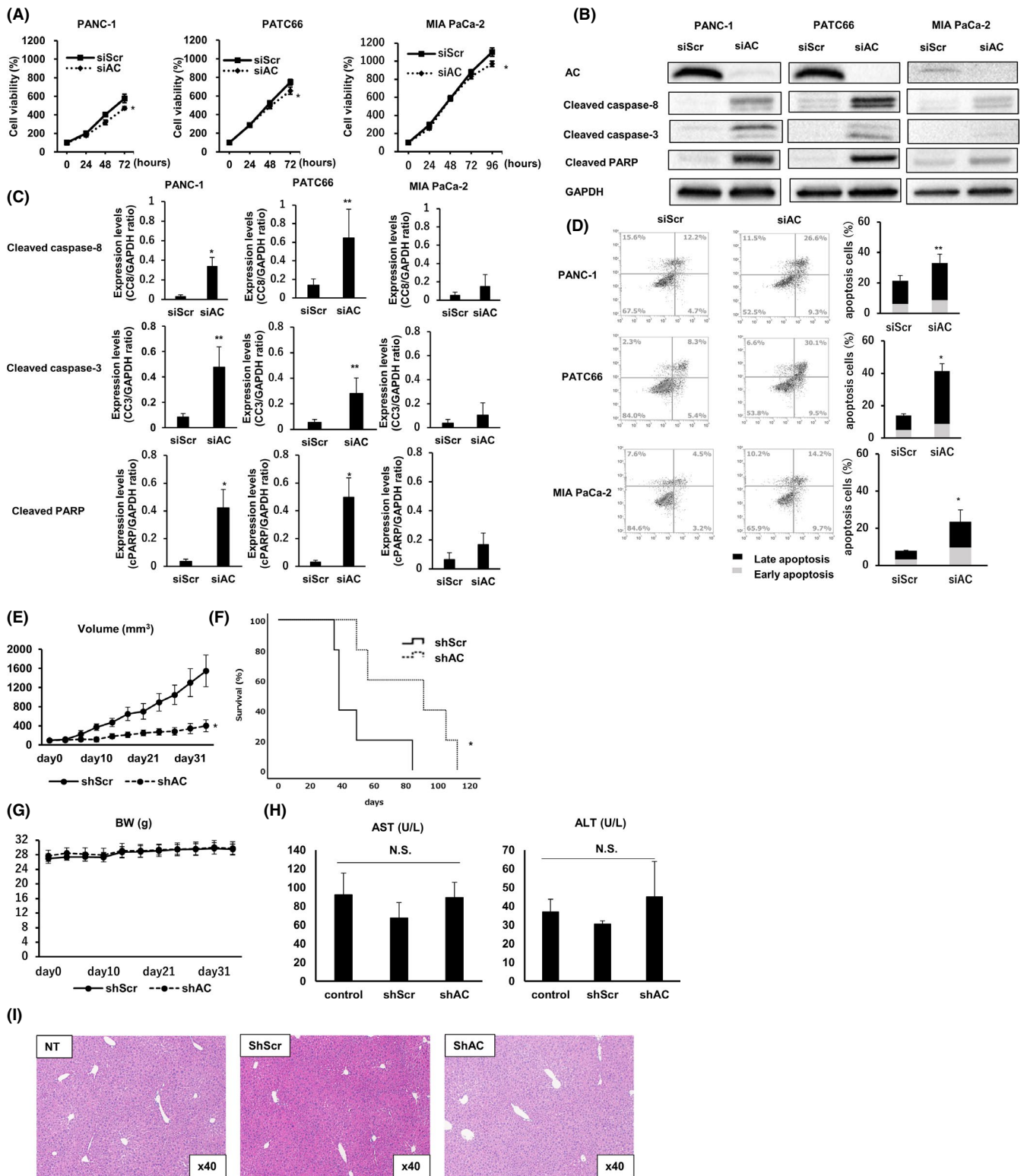
To evaluate whether AC suppression and GEM, a standard drug for pancreatic cancer, have additive antitumor activities, cell proliferation and apoptosis were evaluated under the following two conditions: siScr + GEM and siAC + GEM. The results revealed that siAC +

GEM reduced proliferation in all cell lines (Figure 4A). The results of western blot analyses showed that siAC + GEM enhanced the levels of the apoptosis markers (Figure 4B,C). Furthermore, the annexin assay revealed that siAC + GEM promoted cell apoptosis (Figure 4D). Collectively, these findings show that AC suppression and GEM have additive antitumor effects.

4 | DISCUSSION

In the present study, gene therapy targeting AC had antitumor effects not only in pancreatic cancer cells but also in tumors in a pancreatic cancer xenograft mouse model. Moreover, AC inhibition elicited mitochondrial dysfunction, ROS accumulation, and MnSOD suppression, which resulted in apoptosis of pancreatic cancer cells accompanied by ceramide accumulation (Figure 5). To the best of our knowledge, this is the first report of the mechanisms underlying the antitumor effects induced by AC inhibition in pancreatic cancer cells. It presents a potential therapeutic strategy using the AAV8 vector to inhibit AC.

Ceramide is known to induce cell death and tumor suppression through several mechanisms, such as endoplasmic reticulum stress,



cell cycle arrest, and mitochondria-mediated apoptosis.²⁹ With regard to mitochondria-mediated apoptosis, ceramide activates Bcl-2 family proteins, which exist on the mitochondrial outer membrane, resulting in alterations to mitochondrial outer membrane permeability and ROS accumulation.³⁰ Our data revealed that AC inhibition induced ceramide accumulation, mitochondrial membrane depolarization, and ROS accumulation. Next, MnSOD activities were

evaluated, as this enzyme degrades ROS, especially that localized in the mitochondria. Western blot analysis revealed that AC inhibition decreased MnSOD levels (Figure 3F). Reactive oxygen species accumulation is known to decrease MnSOD expression through Akt activation.²⁸ Moreover, our data indicated the activation of Akt (Figure 3F). These results show that AC inhibition induced mitochondrial dysfunction and decreased MnSOD expression, which resulted

FIGURE 2 Inhibition of acid ceramidase (AC) suppressed cell viability and induced cell apoptosis. A, Cell viability was decreased in the siRNA against AC (siAC) group after 72 h ($*P < .01$; $n = 4$). B, C, Western blot analysis showed that protein expression levels of apoptosis markers were enhanced in the siAC group after 72 h ($*P < .01$; $**P < .05$; $n = 3$). D, Flow cytometry using an annexin V/FITC kit revealed an increase in apoptotic cells in the siAC group after 72 h (PANC-1, $21.4\% \pm 3.5\%$ vs $33.1\% \pm 5.9\%$; PATC66, $14.0\% \pm 1.1\%$ vs $41.4\% \pm 4.7\%$; MIA PaCa-2, $8.0\% \pm 0.3\%$ vs $23.6\% \pm 6.4\%$; $*P < .01$; $**P < .05$; $n = 4$). Inhibition of AC using the adeno-associated virus serotype 8 (AAV8)-shAC vector induced antitumor effects in mice. E, Tumor growth was significantly suppressed in the AAV8-shAC group (AAV8-shScr vs AAV8-shAC, 1546 ± 741 vs 399 ± 281 mm³; $*P < .05$; $n = 5$). F, Overall survival was significantly prolonged in the AAV8-shAC group ($*P < .05$; $n = 5$). Day 0 was defined as the day of AAV8 injection into the tumors. G, There was no difference in the body weight between the AAV8-shScr and AAV8-shAC groups ($n = 5$). H, There were no significant differences in the liver enzyme levels (aspartate aminotransferase [AST] and alanine aminotransferase [ALT]) among the control (nontreatment), AAV8-shScr, and AAV8-shAC groups (control, $n = 3$; AAV8-shScr and shAC, $n = 5$). I, H&E staining of the liver. There was no difference among the groups. N.S, not significant; NT, no treatment

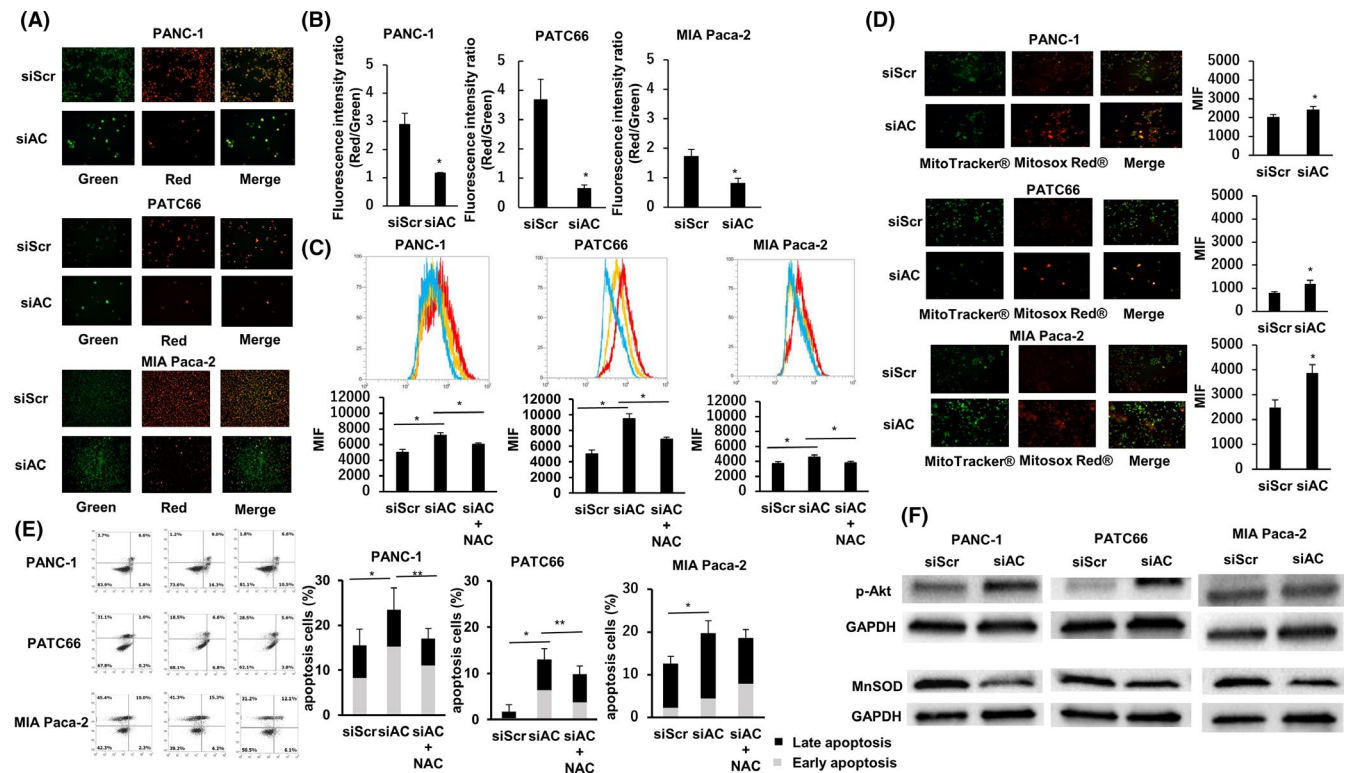


FIGURE 3 A, Mitochondrial membrane potential (MMP) analysis by fluorescence microscopy after 72 h. In each cell line, green fluorescence, which revealed abnormally decreased membrane potential, was enhanced, and red fluorescence, which represented normal membrane potential, was weakened by siRNA against acid ceramidase (siAC), indicating decreased MMP. B, Quantitative analysis of MMP. The red / green fluorescence ratio was decreased in the siAC group ($*P < .01$; $n = 3$). C, Quantitative analysis of intracellular reactive oxygen species (ROS) assessed by flow cytometry (blue, scrambled siRNA [siScr]; yellow, siScr + N-acetylcysteine [NAC]; red, siAC). Intracellular ROS was increased by AC suppression and reduced by NAC ($*P < .01$; $n = 3$). Quantitative assessment of the mean intensity of fluorescence (MIF). D, Analysis of mitochondria-derived ROS assessed by fluorescence microscopy and quantitative analysis by flow cytometry. Mitochondria were stained with MitoTracker, which revealed green fluorescence, and mitochondria-derived ROS were stained with MitoSOX Red, which showed red fluorescence. Red fluorescence was increased and colocalized with green fluorescence in the siAC group, which suggested that mitochondria-derived ROS were increased in the siAC group ($*P < .05$; $n = 3$). E, Flow cytometry using the annexin V/FITC kit revealed increased apoptosis in the siAC group (PANC-1, $15.6\% \pm 3.5\%$ vs $23.4\% \pm 4.8\%$; PATC66, $1.7\% \pm 1.5\%$ vs $13\% \pm 2.4\%$; MIA PaCa-2, $12.6\% \pm 1.7\%$ vs $19.7\% \pm 2.9\%$), which was reduced in the siAC + NAC group (PANC-1, $23.4\% \pm 4.8\%$ vs $17.0\% \pm 2.2\%$; PATC66, $13\% \pm 2.4\%$ vs $9.8\% \pm 1.8\%$; MIA PaCa-2, $19.7\% \pm 2.9\%$ vs $18.7\% \pm 1.9\%$; $*P < .01$; $**P < .05$; $n = 6$). F, Western blot analysis revealed increased p-Akt levels and decreased manganese superoxide dismutase (MnSOD) levels in the siAC group

in ROS accumulation. In addition, NAC counteracted ROS-induced cell apoptosis (Figure 3C,E), indicating that ROS generation is a direct cause of cell apoptosis. A previous study of pancreatic cancer reported that AC inhibition decreased cell growth, although the cytotoxic mechanism was unclear.³¹ Therefore, the current study is the

first to partially elucidate the mechanism underlying apoptosis of pancreatic cancer cells induced by AC inhibition.

Acid ceramidase inhibitors have antitumor effects, although most have been evaluated only in preclinical studies.⁸ Carmofur, which is the only AC inhibitor approved for clinical use,¹⁹ partially crosses the

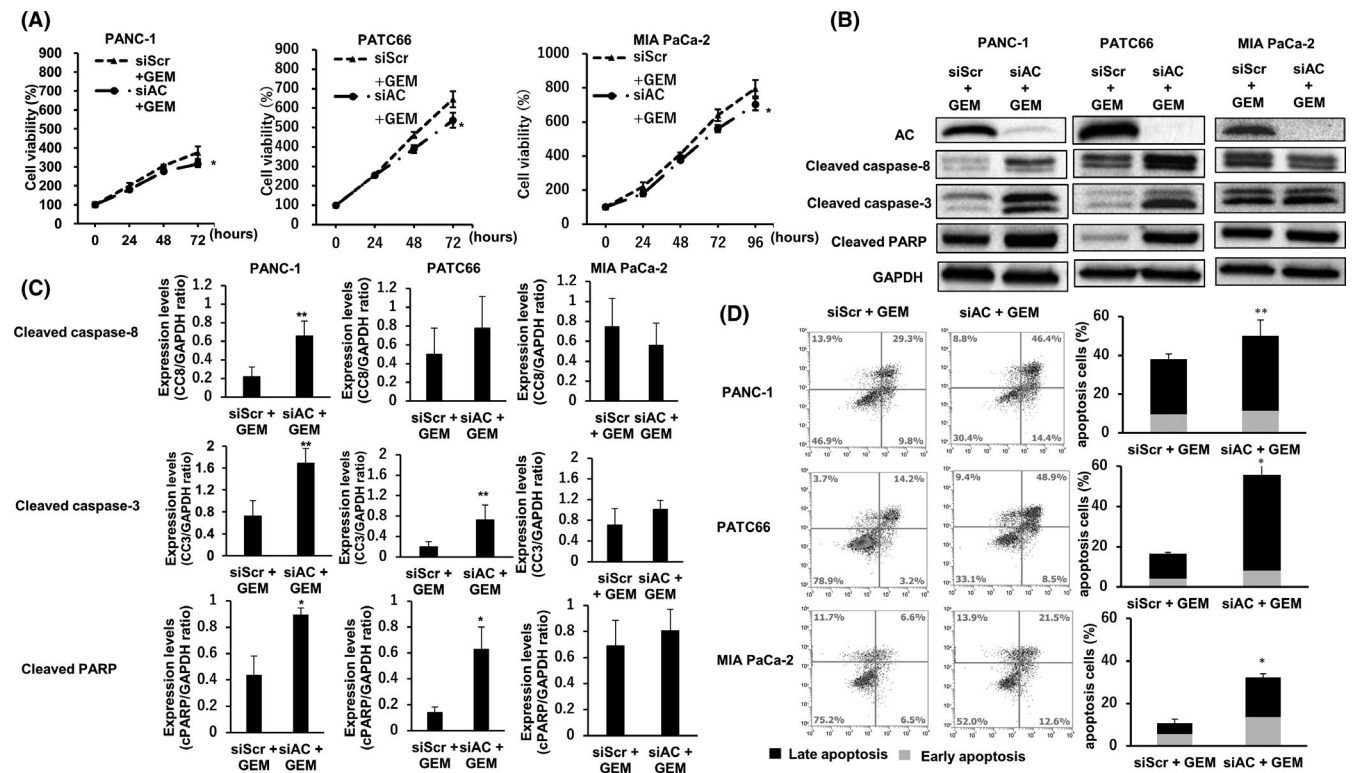


FIGURE 4 Acid ceramidase (AC) inhibition and gemcitabine (GEM) have additive antitumor effects. The concentrations of GEM were as follows: PANC-1, 1 μ mol/L; PATC66, 80 nmol/L; MIA PaCa-2, 0.5 μ mol/L. A, Cell viability was decreased in the siRNA against AC (siAC) + GEM group ($*P < .01$; $n = 4$). B, C, Western blot analysis showed that expressions levels of apoptosis markers were enhanced in the siAC + GEM group ($*P < .01$; $**P < .05$; $n = 3$). D, Flow cytometry using the annexin V/FITC kit revealed increased apoptosis in the siAC + GEM group (PANC-1, 38.0% \pm 2.8% vs 50.2% \pm 8.0%; PATC66, 16.7% \pm 0.5% vs 55.7% \pm 4.5%; MIA PaCa-2, 10.8% \pm 1.8% vs 32.3% \pm 1.8%; $*P < .01$; $**P < .05$; $n = 4$)

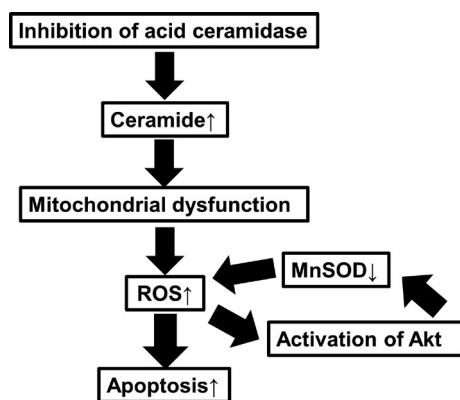


FIGURE 5 Summary scheme showing the mechanism of apoptosis through acid ceramidase (AC) inhibition in pancreatic cancer cells. Inhibition of AC elicited ceramide-induced mitochondrial dysfunction, reactive oxygen species (ROS) accumulation, and manganese superoxide dismutase (MnSOD) suppression, resulting in cell apoptosis

blood-brain barrier, which increases the risk for leukoencephalopathy. As the safety of carmofur is uncertain, a new administration method is required for clinical application as part of an effective therapeutic strategy to inhibit AC. Therefore, a novel AC inhibitor that is both soluble and safe is needed. The AAV vector has potential

for cancer gene therapy,^{32,33} largely due to the lack of apparent pathogenicity,³⁴ which could overcome the safety and insolubility issues of AC inhibitors. The various AAV serotypes have different characteristics.³⁵ Among them, the AAV8 vector is reported to be highly useful for delivery to the pancreas.³⁶ Hence, we investigated the antitumor effect of AC inhibition using the AAV8 vector in a pancreatic cancer xenograft mouse model. Our data revealed that AC inhibition by the AAV8 vector significantly suppressed tumor growth and prolonged overall survival (Figure 2E,F). As the AAV8 vector also has high transduction efficiency in the liver,³⁵ we analyzed the liver enzymes AST and ALT and pathological status to evaluate the potential side-effects. The results revealed no significant changes in AST, ALT, pathological tissue status, or body weight among the non-treatment control, AAV8-shScr, and AAV8-shAC groups (Figure 2G-I), suggesting that AC inhibition by the AAV8 vector did not result in obvious side-effects. The animal experiments revealed that AC inhibition by the AAV8 vector could be useful as a therapeutic strategy against pancreatic cancer. In the current study, we used local injection of AAV8. However, a suitable delivery method will be required to deliver the AAV8 to the cancer cells clinically. To overcome this problem, creating AAV8 with high specificity to cancer cells is one of our future challenges.

The antitumor effects of the combination of AC inhibition and GEM, a standard drug for the treatment of pancreatic cancer, were

also investigated. Our data revealed that the combination of AC inhibition and GEM was superior to GEM alone (Figure 4), indicating that the combination of GEM and AC inhibition using the AAV8 vector could be useful for the treatment of pancreatic cancer.

In conclusion, the results of the present study showed that AC inhibition elicits mitochondrial dysfunction and ROS accumulation, resulting in cell apoptosis accompanied by ceramide accumulation. Moreover, AC inhibition by the AAV8 vector could be a novel therapeutic option for pancreatic cancer.

ACKNOWLEDGMENTS

None.

DISCLOSURE

The authors declare that they have no competing interest.

ORCID

Tomohiko Taniai  <https://orcid.org/0000-0001-8911-5530>

Yoshihiro Shirai  <https://orcid.org/0000-0002-4907-0101>

Ryoga Hamura  <https://orcid.org/0000-0003-1670-4435>

Mitsuru Yanagaki  <https://orcid.org/0000-0003-0664-5830>

Naoki Takada  <https://orcid.org/0000-0003-3192-7979>

Koichiro Haruki  <https://orcid.org/0000-0002-1686-3228>

Kenei Furukawa  <https://orcid.org/0000-0002-5081-6417>

Shu Shimada  <https://orcid.org/0000-0002-4962-0636>

Shinji Tanaka  <https://orcid.org/0000-0002-7718-3453>

Toru Ikegami  <https://orcid.org/0000-0001-5792-5045>

REFERENCES

1. Pralhada Rao R, Vaidyanathan N, Rengasamy M, Mammen Oommen A, Somaiya N, Jagannath MR. Sphingolipid metabolic pathway: an overview of major roles played in human diseases. *J Lipids*. 2013;2013:178910.
2. Ponnusamy S, Meyers-Needham M, Senkal CE, et al. Sphingolipids and cancer: ceramide and sphingosine-1-phosphate in the regulation of cell death and drug resistance. *Future Oncol*. 2010;6:1603-1624.
3. Modrak DE, Gold DV, Goldenberg DM. Sphingolipid targets in cancer therapy. *Mol Cancer Ther*. 2006;5:200-208.
4. Che J, Huang Y, Xu C, Zhang P. Increased ceramide production sensitizes breast cancer cell response to chemotherapy. *Cancer Chemother Pharmacol*. 2017;79:933-941.
5. Kosaka N, Iguchi H, Hagiwara K, Yoshioka Y, Takeshita F, Ochiya T. Neutral sphingomyelinase 2 (nSMase2)-dependent exosomal transfer of angiogenic microRNAs regulate cancer cell metastasis. *J Biol Chem*. 2013;288:10849-10859.
6. Coant N, Hannun YA. Neutral ceramidase: advances in mechanisms, cell regulation, and roles in cancer. *Adv Biol Regul*. 2019;71:141-146.
7. Gebai A, Gorelik A, Li Z, Illes K, Nagar B. Structural basis for the activation of acid ceramidase. *Nat Commun*. 2018;9:1621.
8. Govindarajah N, Clifford R, Bowden D, Sutton PA, Parsons JL, Vimalachandran D. Sphingolipids and acid ceramidase as therapeutic targets in cancer therapy. *Crit Rev Oncol Hematol*. 2019;138:104-111.
9. Cho SM, Kwon HJ. Acid ceramidase, an emerging target for anti-cancer and anti-angiogenesis. *Arch Pharm Res*. 2019;42:232-243.
10. Farber S. A lipid metabolic disorder: disseminated lipogranulomatosis; a syndrome with similarity to, and important difference from, Niemann-Pick and Hand-Schüller-Christian disease. *AMA Am J Dis Child*. 1952;84:499-500.
11. Mahdy AEM, Cheng JC, Li J, et al. Acid ceramidase upregulation in prostate cancer cells confers resistance to radiation: AC inhibition, a potential radiosensitizer. *Mol Ther*. 2009;17:430-438.
12. Roh JL, Park JY, Kim EH, Jang HJ. Targeting acid ceramidase sensitises head and neck cancer to cisplatin. *Eur J Cancer*. 2016;52:163-172.
13. Doan NB, Alhajala H, Al-Gizawiy MM, et al. Acid ceramidase and its inhibitors: a de novo drug target and a new class of drugs for killing glioblastoma cancer stem cells with high efficiency. *Oncotarget*. 2017;8:112662-112674.
14. Giovannetti E, Leon LG, Bertini S, et al. Study of apoptosis induction and deoxycytidine kinase/cytidine deaminase modulation in the synergistic interaction of a novel ceramide analog and gemcitabine in pancreatic cancer cells. *Nucleos Nucleot Nucl Acids*. 2010;29:419-426.
15. Realini N, Solorzano C, Pagliuca C, et al. Discovery of highly potent acid ceramidase inhibitors with in vitro tumor chemosensitizing activity. *Sci Rep*. 2013;3:1035.
16. Bai A, Mao C, Jenkins RW, Szulc ZM, Bielawska A, Hannun YA. Anticancer actions of lysosomally targeted inhibitor, LCL521, of acid ceramidase. *PLoS One*. 2017;12:e0177805.
17. Realini N, Palese F, Pizzirani D, et al. Acid ceramidase in melanoma: expression, localization, and effects of pharmacological inhibition. *J Biol Chem*. 2016;291:2422-2434.
18. Sakamoto J, Hamada C, Rahman M, et al. An individual patient data meta-analysis of adjuvant therapy with capecitabine in patients with curatively resected colon cancer. *Jpn J Clin Oncol*. 2005;35:536-544.
19. Nguyen HS, Awad AJ, Shabani S, Doan N. Molecular targeting of acid ceramidase in glioblastoma: a review of its role, potential treatment, and challenges. *Pharmaceutics*. 2018;10(2):45.
20. Yamamoto M, Arai S, Sugahara K, Tobe T. Adjuvant oral chemotherapy to prevent recurrence after curative resection for hepatocellular carcinoma. *Br J Surg*. 1996;83:336-340.
21. Ueda N, Yamanaka K, Yamamoto S. Purification and characterization of an acid amidase selective for N-palmitoylethanolamine, a putative endogenous anti-inflammatory substance. *J Biol Chem*. 2001;276:35552-35557.
22. Tsuboi K, Sun YX, Okamoto Y, Araki N, Tonai T, Ueda N. Molecular characterization of N-acyl ethanolamine-hydrolyzing acid amidase, a novel member of the cholesteryl glycerophosphorylcholine hydrolase family with structural and functional similarity to acid ceramidase. *J Biol Chem*. 2005;280:11082-11092.
23. Shirai Y, Uwagawa T, Shiba H, et al. Recombinant thrombomodulin suppresses tumor growth of pancreatic cancer by blocking thrombin-induced PAR1 and NF-kappaB activation. *Surgery*. 2017;161:1675-1682.
24. Tea MN, Poonnoose SI, Pitson SM. Targeting the sphingolipid system as a therapeutic direction for glioblastoma. *Cancers*. 2020;12(1):111.
25. Ogretmen B. Sphingolipid metabolism in cancer signalling and therapy. *Nat Rev Cancer*. 2018;18:33-50.
26. Arora AS, Jones BJ, Patel TC, Bronk SF, Gores GJ. Ceramide induces hepatocyte cell death through disruption of mitochondrial function in the rat. *Hepatology*. 1997;25:958-963.
27. Kudryavtseva AV, Krasnov GS, Dmitriev AA, et al. Mitochondrial dysfunction and oxidative stress in aging and cancer. *Oncotarget*. 2016;7:44879-44905.
28. Nogueira V, Park Y, Chen C-C, et al. Akt determines replicative senescence and oxidative or oncogenic premature senescence and sensitizes cells to oxidative apoptosis. *Cancer Cell*. 2008;14:458-470.
29. Nganga R, Oleinik N, Ogretmen B. Mechanisms of ceramide-dependent cancer cell death. *Adv Cancer Res*. 2018;140:1-25.
30. Ueda N. Ceramide-induced apoptosis in renal tubular cells: a role of mitochondria and sphingosine-1-phosphate. *Int J Mol Sci*. 2015;16:5076-5124.

31. Morad SAF, Messner MC, Levin JC, et al. Potential role of acid ceramidase in conversion of cytostatic to cytotoxic end-point in pancreatic cancer cells. *Cancer Chemother Pharmacol*. 2013;71:635-645.
32. Santiago-Ortiz JL, Schaffer DV. Adeno-associated virus (AAV) vectors in cancer gene therapy. *J Control Release*. 2016;240:287-301.
33. Pinto C, Silva G, Ribeiro AS, et al. Evaluation of AAV-mediated delivery of shRNA to target basal-like breast cancer genetic vulnerabilities. *J Biotechnol*. 2019;300:70-77.
34. Daya S, Berns KI. Gene therapy using adeno-associated virus vectors. *Clin Microbiol Rev*. 2008;21:583-593.
35. Wu Z, Asokan A, Samulski RJ. Adeno-associated virus serotypes: vector toolkit for human gene therapy. *Mol Ther*. 2006;14:316-327.
36. Wang AY, Peng PD, Ehrhardt A, Storm TA, Kay MA. Comparison of adenoviral and adeno-associated viral vectors for pancreatic gene delivery in vivo. *Hum Gene Ther*. 2004;15:405-413.

SUPPORTING INFORMATION

Additional supporting information may be found online in the Supporting Information section.

How to cite this article: Taniai T, Shirai Y, Shimada Y, et al. Inhibition of acid ceramidase elicits mitochondrial dysfunction and oxidative stress in pancreatic cancer cells. *Cancer Sci*. 2021;112:4570–4579. <https://doi.org/10.1111/cas.15123>